Downloaded from rsta.royalsocietypublishing.org

PHILOSOPHICAL TRANSACTIONS OF THE ROYAL SOCIETY A MATHEMATICAL, PHYSICAL & ENGINEERING SCIENCES

Radioactive ion beams in solid state physics

Doris Forkel-Wirth

Phil. Trans. R. Soc. Lond. A 1998 **356**, 2137-2162
doi: 10.1098/rsta.1998.0266

Email alerting service Receive free email alerts when new articles cite this article - sign up in the box at the top right-hand corner of the article or click **here**

To subscribe to *Phil. Trans. R. Soc. Lond. A* go to: **http://rsta.royalsocietypublishing.org/subscriptions**

This journal is © 1998 The Royal Society

Downloaded from rsta.royalsocietypublishing.org

PHILOSOPHICAL TRANSACTIONS OF THE ROYAL SOCIETY A MATHEMATICAL, PHYSICAL & ENGINEERING SCIENCES

The Royal Society

Radioactive ion beams in solid state physics

By Doris Forkel-Wirth
CERN/PPE, CH-1211 Geneva 23, Switzerland

The use of radioactive beams in solid state physics has become more and more popular during the past few years, and both off-line and on-line mass separators are used for implanting various types of radioactive isotopes into the material under investigation. Besides the nuclear techniques of Mössbauer spectroscopy, perturbed angular correlation spectroscopy, β-NMR, or the ion-beam technique of emission channelling, a new group of radiotracer techniques has been established, which combines radioactive probe atoms with conventional semiconductor physics methods such as deep-level transient spectroscopy, capacitance–voltage measurements, Hall-effect measurements, or photoluminescence spectroscopy.

This paper aims to give an idea of the potential of modern 'radioactive solid state physics' by describing some typical experiments.

Keywords: perturbed angular correlation spectroscopy; ion implantation; semiconductors; defects; impurities; hydrogen; transmutation doping; radiotracer diffusion

1. Introduction

The application of radioactive isotopes in solid state physics research dates back almost 80 years, when early radiotracer diffusion experiments were performed to study the self-diffusion of lead atoms in lead (Groh & Hevesey 1920). Many years later, in 1957, the Mössbauer effect, i.e. the resonant, recoilless emission and absorption of γ-rays was discovered (Mössbauer 1958*a*, *b*), and its importance for solid state physics immediately became evident (Boyle & Hall 1962). In the mid-1960s, the first emission channelling (EC) experiments (Uggerhoj 1966) on single crystals doped with radioactive isotopes followed. Hyperfine techniques, such as perturbed angular correlation (PAC) spectroscopy (Aeppli *et al*. 1950; Deutsch 1951) and β-NMR (Connor 1959), had already served for many decades in nuclear physics to determine key nuclear properties like magnetic or quadrupole moments of excited nuclear states before they were successfully applied in solid state physics (Haas & Shirley 1973; Christiansen *et al*. 1976; McDonald & McNab 1976) from the 1970s onwards. One common feature of all these nuclear solid state physics techniques is that they are based on the detection of the radioactive decay products (α-, β-particles, γ-rays), which carry information about the lattice sites, dynamics, microscopic and electronic structure of the very specific probe atoms from which they are emitted.

Since the early 1990s a new group of radiotracer techniques has been introduced by combining traditional semiconductor physics methods, such as deep-level transient spectroscopy (DLTS) (Petersen & Nielsen 1990, 1992), capacitance–voltage (CV) measurements (Bollmann *et al*. 1996*a*, *b*), Hall-effect (HE) measurements (Gwilliam *et al*. 1992), photoluminescence spectroscopy (PLS) (Magerle 1995; Daly *et al*. 1995;

© 1998 The Royal Society
TEX Paper

Downloaded from rsta.royalsocietypublishing.org

Henry *et al*. 1996), or electron paramagnetic resonance spectroscopy (EPRS) (Burchard *et al*. 1996, 1997*a*) with radioactive isotopes. All these very powerful techniques are commonly used to investigate the structural, electronic and optical properties of point defects in semiconductors. With the exception of EPRS, all these techniques are only able to assign observed signals, and hence properties such as the electronic levels, more or less indirectly to the corresponding defect or impurity. The tracer techniques, however, employ radioactive atoms (normally β-emitters) and overcome the chemical blindness by labelling the impurity under study via its radioactive decay constant. In β-decay, the chemical nature of the isotope changes and the impurity transmutes from one chemical element into another, thus changing its electronic and optical properties. Therefore, it is already sufficient to record the time dependence of the signals over a period adapted to the half-life of the isotope. When the change in the signals follows the radioactive decay, i.e. the signal related to the mother isotope decreases and that of the daughter increases, then the chemical nature of the impurities is unambiguously identified.

Until now, approximately 100 different radioactive isotopes have been used in nuclear solid state physics, ranging from ^{8}Li up to ^{213}Fr. They are produced by nuclear reactions in reactors or at accelerators, and the doping of the host lattice is performed either by a nuclear reaction inside the material, by recoil implantation, or by diffusion or implantation after nuclear production and chemical separation. However, the most versatile tool is represented by an on-line isotope mass separator like ISOLDE (Kugler 1993), which offers nearly an unlimited applicability. It provides a wide range of various radioactive isotopes, which in many cases cannot be produced elsewhere. The combination of chemically selective ion sources and high-mass resolution results in an isotopically clean ion beam that is free of contamination. Nearly all combinations of probe atoms and host lattices are possible, since the isotopes can be produced and implanted within a few seconds into any host lattice. Therefore, even very short-lived isotopes such as ^{8}Li, with a half-life of only 840 ms, can be used for EC or β-NMR.

Nuclear techniques employ the radioactive nuclei as probes of their structural or electronic lattice environment either in metals (Lindroos *et al*. 1992), insulators (Restle *et al*. 1995), semiconductors or superconductors (Correia *et al*. 1996), on surfaces (Lohmüller *et al*. 1996; Granzer *et al*. 1996; Bertschat *et al*. 1997), interfaces or even in complex biomolecules (Butz 1993). However, a major part of these activities is focused on the investigation of defects and impurities in semiconductors like Si, Ge, III–V or II–VI compounds. Among the main topics of investigation are implantation-induced lattice damage and its annealing behaviour, the lattice site of the implanted ion after annealing, the interaction between impurities or between impurities and intrinsic defects, the electronic and optical properties of the implanted species and the identification of defects and impurities.

This paper gives an overview of the potential of nuclear techniques by describing some typical experiments. Most often, several techniques have to be applied before a final understanding of the physical problem under study can be achieved. This will be demonstrated for combined EC, PAC and HE annealing studies of GaAs following implantation with low-energy heavy ions. PAC results on hydrogen passivation and hydrogen diffusion in III–V semiconductors yield information on an atomic scale that cannot be obtained in any other way. Investigations of the Au diffusion in amorphous Si very efficiently exploit the unique possibilities of ISOLDE and provide

PHILOSOPHICAL TRANSACTIONS OF THE ROYAL SOCIETY A MATHEMATICAL, PHYSICAL & ENGINEERING SCIENCES

PHILOSOPHICAL TRANSACTIONS OF THE ROYAL SOCIETY A MATHEMATICAL, PHYSICAL & ENGINEERING SCIENCES

Downloaded from rsta.royalsocietypublishing.org

PHILOSOPHICAL TRANSACTIONS OF THE ROYAL SOCIETY A MATHEMATICAL, PHYSICAL & ENGINEERING SCIENCES

a new insight into trap-retarded diffusion mechanisms. Recently, it could be proven that combining common techniques like DLTS or PLS with radioactive isotopes yield new, unexpected information, even in the case of well-known systems like Au and Pt in Si. Furthermore, transmutation doping was successfully used at ISOLDE for site-selective doping of III–V and II–VI semiconductors. Finally, it will be stated that the availability of future medium-energy radioactive beams will certainly boost radioactive solid state physics.

2. Techniques

Before presenting exemplary experiments in detail, some of the techniques are described briefly. A compilation of most of the nuclear techniques can be found in Schatz *et al*. (1996).

Perturbed angular correlation (PAC) and *Mössbauer spectroscopy* (MS) are very well suited to the investigation of the structural, dynamical and electronic properties of single impurities, inter-impurity and impurity-defect complexes on an atomic scale. PAC and MS are based on the observation of the electric or magnetic hyperfine interaction between the nuclear moments of a specific probe nucleus and the magnetic or electric fields induced by its surroundings (Frauenfelder & Steffen 1965). Besides the magnetic hyperfine interaction, both PAC and MS detect the electric quadrupole hyperfine interaction between the nuclear quadrupole moment Q of a specific probe atom and the electric field gradient (EFG) which is caused by the deviation of the electric charge distribution around the probe atom from cubic or tetrahedral symmetry. The magnetic as well as the electrical quadrupole hyperfine interaction results in a splitting of the m-sublevels of the corresponding nuclear level. In addition, MS is able to monitor the Coulomb interaction between the electrical charge distribution of the nuclei and that of the s-electrons. This interaction does not contribute to the splitting of the m-sublevels, but results in a relative shift of the energy levels.

MS experiments detect the hyperfine interaction, i.e. the isomer shift and the splitting of the Mössbauer level by monitoring its de-excitation into the ground state. Commonly, the energy of the γ-quanta emitted by the Mössbauer nuclei are directly measured by resonance-absorption experiments.

PAC experiments such as MS require very specific probe atoms. The PAC probe atom decays by a $\gamma\gamma$-cascade via an isomeric nuclear state. The hyperfine interaction is detected by $\gamma\gamma$-coincidence measurements, where the time-delayed coincidence spectra are combined to form the so called $R(t)$ spectra. Each EFG is characterized by a specific time modulation of the coincidence and $R(t)$ spectra, respectively. In diamond- or zinc-blende lattices, like Si or III–V compounds, the appearance of an EFG is either due to probe atoms located on non-substitutional or non-ideal tetrahedral lattice sites or due to the trapping of impurities or defects at the probe atoms.

Emission channelling uses the channelling or blocking effect of charged particles emitted from radioactive isotopes in single crystals to determine the lattice site of the probe atoms. The α- or β-particles are detected in different directions with respect to the crystal lattice, and the angular dependence of the counting rate clearly indicates whether the probe atom occupies an interstitial or substitutional lattice site. A detailed description is given in Hofsäss & Lindner (1991).

Downloaded from rsta.royalsocietypublishing.org

PHILOSOPHICAL TRANSACTIONS OF THE ROYAL SOCIETY A MATHEMATICAL, PHYSICAL & ENGINEERING SCIENCES

Capacitance–voltage (CV) measurements and *deep-level transient spectroscopy* (DLTS) are both electrical techniques based on the measurement of the capacitance of the depletion zone of a Schottky junction. CV yields the spatial distribution and concentration of deep and shallow dopants (Sze 1981), whereas DLTS determines in addition the energy level of deep impurities and their capture cross-sections for electrons and holes (Lang 1974*a*, *b*).

Photoluminescence spectroscopy (PLS) is an optical technique where electrons and holes in semiconductors are generated by optical pumping, usually with a laser. The electrons and holes recombine via different channels, for example, by interband transitions between valence and conduction band or by transitions via an impurity state. For radiative transitions, the energy of the recombinations observed by PLS gives information on the electrical and optical properties of defects and impurities (Sze 1981; Lightowlers 1990).

Radiotracer diffusion requires the incorporation of radioactive atoms into the sample either by diffusion or implantation. After doping, the samples are heated to activate the diffusion and subsequently sectioned, for example, by Ar^+-beam sputtering. The diffusion profile is deduced by monitoring the X- and γ-rays emitted by the radiotracers left in the samples after sectioning. By applying this technique, diffusion profiles with nanometre resolution can be deduced.

3. Implantation-induced radiation damage and its annealing behaviour in III–V semiconductors

For nearly all 'radioactive' solid state physics methods implanting the radioactive ions into the material under study by off- and on-line mass separators represents the ideal doping technique for the following reasons.

1. In ion implantation, numerous combinations of host lattices and probe atoms are possible.

2. Ion implantation, in particular by on-line separators, enables the use of short-lived isotopes, whereas doping techniques like diffusion are limited to radioisotopes with half-lives of the order of days and longer. In addition, diffusion might be hampered by surface barrier problems, by low diffusion coefficients and the elevated diffusion temperatures may cause a degradation of the material, particularly of multicomponent systems.

3. The clean ion beam obtained by combining chemically selective ion sources and mass separation avoids co-implantations of unwanted impurities.

On the other hand, the radiation damage induced by ion implantation causes a major problem. Thus, before being able to perform any other experiment, it is vital to know that the radiation damage has been removed, to identify the lattice site of the implanted atom, and to investigate the contribution of the dopants to the electrical properties of the semiconductor.

In the following, the results from several techniques (EC, PAC, Hall measurements) on the annealing behaviour of radiation defects and the electrical activation of Cd impurities in GaAs after implantation at ISOLDE are described. At first glance the data from the three different techniques seem to be contradictory, and each of

Downloaded from rsta.royalsocietypublishing.org

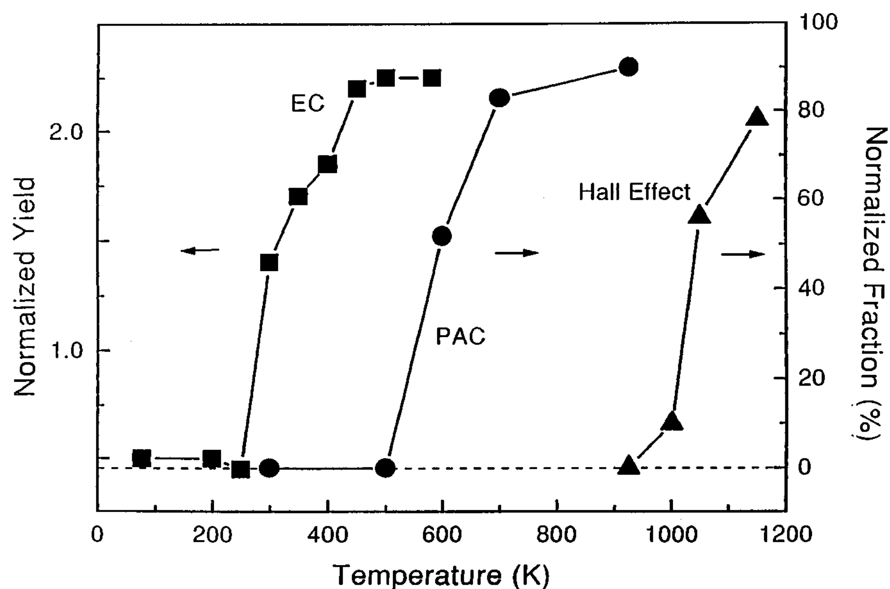

Figure 1. Annealing behaviour of GaAs after Cd implantation as observed by EC, PAC and HE measurements. The left y-axis refers to the normalized yield of the channelling effect for substitutional Cd atoms as taken from Hofsäss *et al.* (1992). The right y-axis refers to the fraction of Cd probe atoms on unperturbed, substitutional lattice sites (PAC) and the fraction of electrically active Cd acceptors (Hall) as taken from Pfeiffer *et al.* (1991*a*) and Moriya *et al.* (1993).

these techniques seems to favour a different 'annealing temperature' to remove the implantation damage. However, the combination of the findings of all the different methods allows one to solve the puzzle and to obtain a complete picture.

All the experiments were performed on GaAs samples implanted at ISOLDE with ^{111m}Cd at 60 keV and 300 K, the doses ranging from 10^{12} to 10^{13} atoms cm^{-3}. The projected range R_p and the straggling ΔR_p of the ions as calculated with the TRIM code (Biersack & Haggmark 1980) are 25 nm and 10 nm, respectively, and the resulting Cd peak concentration is of the order of 10^{17}–10^{19} cm^{-3}. EC experiments, after annealing the samples at 450 K, indicate that nearly all Cd atoms have been incorporated on substitutional lattice sites (Winter *et al.* 1990; Hofsäss *et al.* 1992). The same process was extensively investigated by using PAC and HE measurements (Pfeiffer *et al.* 1991*a*; Moriya *et al.* 1993; Deicher & Pfeiffer 1994). From the PAC measurements it was found that at annealing temperatures below 500 K most of the probe atoms are exposed to a distribution of EFG caused by a variety of defects in the neighbourhood. With increasing annealing temperature, the fraction of Cd atoms on unperturbed, substitutional lattice sites increases, and above 700 K nearly all Cd atoms are located on these sites. Over the full range of the annealing temperatures, no trapping of any defect or impurity at the Cd probe atom is observed. The HE measurements (Moriya *et al.* 1993), however, reveal, only after an annealing step at 1050 K, the p-type conductivity expected for Cd acceptors (see figure 1). At lower temperatures the sample is still n-type.

The results of the different techniques are interpreted as follows (Pfeiffer *et al.* 1991*a*; Moriya *et al.* 1993): already after annealing at 500 K nearly all Cd atoms are

Downloaded from rsta.royalsocietypublishing.org

MATHEMATICAL, PHYSICAL & ENGINEERING SCIENCES
PHILOSOPHICAL TRANSACTIONS OF THE ROYAL SOCIETY A

located on substitutional lattice sites, as demonstrated by EC. But the PAC technique shows unperturbed, substitutional lattice sites for all Cd atoms only above 700 K. This is not a discrepancy but is the result of the different sensitivities of the two techniques. EC provides direct information about the lattice sites of the implanted ions as well as about the annealing of *amorphous zones* and *extended defects*. PAC, on the other hand, detects *extended* and *point defects* in the neighbourhood of the probe atom. Although extended defects are already annealed at 500 K, point defects still exist in the neighbourhood of the probe atoms up to 700 K. Above this temperature point defects, which are visible in PAC measurements, are also removed, but the expected p-type conductivity due to the Cd acceptors cannot yet be detected by electrical measurements (HE) and the net conductivity is still n-type. This is due to the coexistence of implantation-induced defects, which act as donors and overcompensate the Cd acceptors. The passivation of Cd acceptors by donors, i.e. the formation of close acceptor–donor pairs, as the reason for the missing p-conductivity, can be ruled out since no trapping of any defect or impurity at the Cd acceptor is observed by PAC. Finally, above 1100 K the electrical measurements reveal a p-type character for the implanted GaAs, indicating that at this temperature the compensating donors are removed.

Similar investigations have been performed on other III–V semiconductors after the implantation of 60 keV ^{111m}Cd atoms (Pfeiffer *et al*. 1991*a*; Moriya *et al*. 1993; Deicher & Pfeiffer 1994; Baurichter *et al*. 1989*a*, *b*, 1991; Forkel-Wirth *et al*. 1994). In all materials (GaAs, InAs, InP, GaP, InSb) the implantation damage could be removed without losing too many probe atoms by out-diffusion, an indispensable requirement for carrying out studies on other topics, such as, for example, the interaction between impurities in III–V semiconductors. For further illustration, PAC experiments on hydrogen passivation and diffusion in III–V semiconductors are described.

4. Hydrogen passivation and diffusion in III–V semiconductors

Hydrogen represents one of the most important impurities in semiconductors (Pankove & Johnson 1991; Pearton 1994), both from the technical and the scientific points of view. During various manufacturing process steps, hydrogen is easily incorporated into the semiconducting material, where it very efficiently interacts with other impurities or defects. Hydrogen either saturates dangling bonds, passivates shallow and deep-level dopants or impurities (Pankove & Johnson 1991; Pearton 1994), or causes new, hydrogen-related electronic levels (Leitch *et al*. 1992; Conibear *et al*. 1993). Hydrogen can be introduced unintentionally during crystal growth (Clerjaud *et al*. 1991), or in many of the subsequent stages of device processing like reactive-ion etching (Pankove & Johnson 1991; Pearton 1994). It appears ionized (H^+, H^-), atomic (H^0), stable molecular (H_2), metastable molecular (H_2^*), or precipitated (H-platelets) (Johnson *et al*. 1991; Pavesi & Giannozzi 1992; van de Walle 1991), and this rather puzzling behaviour poses problems in understanding processes like complex formation and hydrogen diffusion.

(*a*) *Hydrogen passivation in III–V semiconductors*

The concept of hydrogen passivation of donors or acceptors comprises the formation of next-nearest, electrically inactive hydrogen–dopant pairs. Due to the Coulomb

Downloaded from rsta.royalsocietypublishing.org

MATHEMATICAL, PHYSICAL & ENGINEERING SCIENCES
PHILOSOPHICAL TRANSACTIONS OF THE ROYAL SOCIETY A

interaction, H^+ (H^-) ions are trapped at the ionized acceptors A^- (donors D^+). The two different charge states compensate each other, the resulting complexes are electrically inactive, and the resistivity of the semiconductor increases.

Since the late 1980s, many PAC experiments have been carried out on hydrogen in Si (Wichert *et al*. 1987; Baurichter *et al*. 1989*a*, *b*; Gebhard *et al*. 1991) and III–V semiconductors (Deicher & Pfeiffer 1994; Baurichter *et al*. 1992; Forkel-Wirth *et al*. 1994, 1995, 1996; Pfeiffer *et al*. 1991*b*; Burchard *et al*. 1997*b*–*d*), and a considerable amount of new information could be provided concerning formation, microscopic structure and stability of acceptor–hydrogen complexes. PAC studies on acceptor–hydrogen interactions require the doping of the material with probe atoms representing acceptor impurities in the corresponding semiconductor. For Si this demand can easily be fulfilled by using the common PAC probe atom, $^{111}\mathrm{In} \rightarrow {}^{111}\mathrm{Cd}$ ($T_{1/2} = 2.8$ d), and implanting it off-line into the samples. Similar investigations in III–V semiconductors, however, pose a bigger problem, since ^{111}In as a group III element does not represent an electrically active impurity. Fortunately, the PAC probe atom, $^{111m}\mathrm{Cd} \rightarrow {}^{111}\mathrm{Cd}$ ($T_{1/2} = 45$ min), exists, which represents an acceptor in III–V semiconductors and which is available at the on-line mass separator ISOLDE as an isotopically clean ion beam with sufficient high intensity (*ca.* 10^9 atoms s^{-1}).

After ^{111m}Cd implantation and annealing, the III–V semiconductor samples were hydrogenated by two different charging techniques: plasma charging and low-energy H^+ implantation. Whereas the plasma-charging technique might suffer from the coproduction of lattice defects and problems concerning reproducibility, a low-energy and mass-separated proton beam avoids the formation of defects and an unwanted contamination of the samples.

The first hints of hydrogen-correlated complexes formed at the ^{111m}Cd acceptor were obtained after hydrogen *plasma charging* of undoped GaAs and InP (Baurichter *et al*. 1989*a*, *b*). Very soon after, PAC experiments on plasma-charged, undoped InAs and GaP as well as on InSb followed (Baurichter *et al*. 1991, 1992) and well-defined EFGs have been observed in all materials. In GaAs, InAs and InP up to two different EFGs, corresponding to two different H-induced complexes ($f_1(\mathrm{H}), f_2(\mathrm{H})$) were detected, whereas in GaP and InSb only one was found ($f_1(\mathrm{H})$) (see figure 2). All EFG tensors characterizing $f_1(\mathrm{H})$ are axially symmetric and the main axis is orientated in the $\langle 1\,1\,1\rangle$ lattice direction.

In parallel, GaAs, InP, InAs, GaP and very recently GaN were investigated after proton implantation at energies between 150 and 400 eV and doses between 10^{14} and 10^{16} cm^{-2} (Deicher & Pfeiffer 1994; Pfeiffer *et al*. 1991*b*; Burchard *et al*. 1997*b*). In H^+-implanted GaAs, InAs and GaP samples the same configurations ($f_1(\mathrm{H}), f_2(\mathrm{H})$) could be observed as in plasma-charged crystals, but in InP only $f_1(\mathrm{H})$ appeared. Very recent experiments in InAs revealed even the existence of a third hydrogen-correlated complex ($f_2(\mathrm{H})^*$) whose PAC parameters are very similar to those of $f_2(\mathrm{H})$. In GaN, two different hydrogen-correlated complexes ($f_1(\mathrm{H}), f_1(\mathrm{H})^*$) have been found after low-energy H^+ implantation. The PAC data for all hydrogen-correlated complexes are given in table 1. Control experiments in GaAs and InAs after Ar^+ (150 eV, 1×10^{14} cm^{-2}) and He^+ (1 keV, 3×10^{14} cm^{-2}) implantations, respectively, did not reveal the formation of any complex at all (Deicher & Pfeiffer 1994; Forkel-Wirth *et al*. 1995). This very strongly supports an interpretation of $f_1(\mathrm{H})$ and $f_2(\mathrm{H})$ in terms of complexes formed by the trapping of the positively charged donor H^+ at the negatively charged acceptor Cd^-. According to the exper-

Downloaded from rsta.royalsocietypublishing.org

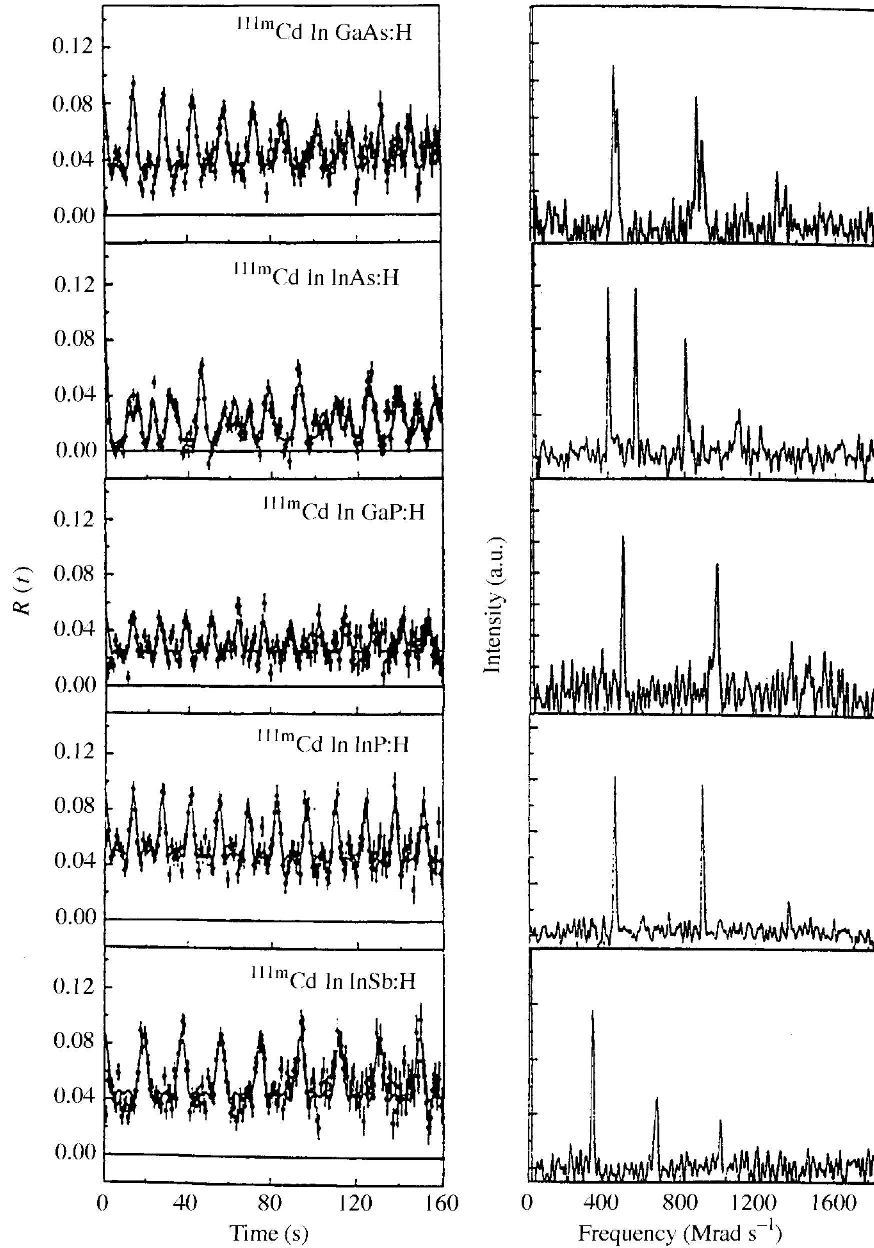

Figure 2. $R(t)$ spectra and the corresponding Fourier transforms of PAC measurements on Cd-doped, plasma-charged III–V semiconductors. The PAC probe atom ^{111m}Cd was used and thus each EFG results in three Fourier peaks. Their relative intensities depend on the orientation of the detectors with regard to the crystallographic axis of the single crystal.

imental findings complex $f_1(\mathrm{H})$ is identified as a Cd–H pair. Its axially symmetric EFG tensor ($\eta = 0$) indicates an axially symmetric complex and the Cd–H pair is the simplest configuration fulfilling this requirement. The $\langle 1\,1\,1 \rangle$ orientation of the EFG

PHILOSOPHICAL TRANSACTIONS OF THE ROYAL SOCIETY A MATHEMATICAL, PHYSICAL & ENGINEERING SCIENCES

PHILOSOPHICAL TRANSACTIONS OF THE ROYAL SOCIETY A MATHEMATICAL, PHYSICAL & ENGINEERING SCIENCES

PHILOSOPHICAL TRANSACTIONS OF THE ROYAL SOCIETY A MATHEMATICAL, PHYSICAL & ENGINEERING SCIENCES
PHILOSOPHICAL TRANSACTIONS OF THE ROYAL SOCIETY A MATHEMATICAL, PHYSICAL & ENGINEERING SCIENCES

Table 1. *PAC parameters of* Cd–H *correlated complexes in III–V semiconductors*
(The PAC measurements were performed by using the PAC probe atom ^{111m}Cd $\rightarrow$ ^{111}Cd.)

material	complex	ν_Q (MHz)	η	orientation	interpretation	references
GaAs	$f_1(H)$	457(2)	0	$\langle 111 \rangle$	Cd–H pair	Baurichter *et al.* 1989*a*; Pfeiffer *et al.* 1991*b*
	$f_2(H)$	479(3)	0	$\langle 111 \rangle$	Cd–H*, not identified	Baurichter *et al.* 1991, 1992
		481(2)				Pfeiffer *et al.* 1991*b*
InAs	$f_1(H)$	427(1)	0	$\langle 111 \rangle$	Cd–H pair	Baurichter *et al.* 1991, 1992; Forkel-Wirth *et al.* 1994
	$f_2(H)$	577(1)	0.09	$\langle 110 \rangle$	Cd–H$_x$ or Cd–H defect complex	Baurichter *et al.* 1991, 1992; Forkel-Wirth *et al.* 1995 Forkel-Wirth *et al.* 1996; Burchard *et al.* 1997*c*
	f_2(H)*	555(1)	0.19	$\langle 110 \rangle$	Cd–H$_x$ or Cd–H defect complex	Burchard *et al.* 1997*c*
InP	$f_1(H)$	485(3)	0	$\langle 111 \rangle$	Cd–H pair	Deicher *et al.* 1994; Baurichter *et al.* 1989*b*; Pfeiffer *et al.* 1991*b*
		484(1)				Baurichter *et al.* 1992
	$f_2(H)$	495(2)	0	$\langle 111 \rangle$	Cd–H*, not identified	Baurichter *et al.* 1992
GaP	$f_1(H)$	525(3)	0	$\langle 111 \rangle$	Cd–H pair	Baurichter *et al.* 1992; Forkel-Wirth *et al.* 1994, 1995
InSb	$f_1(H)$	357(2)	0	?	Cd–H pair (?)	Baurichter *et al.* 1991, 1992
GaN	$f_1(H)$	360(1)	0	$\langle 111 \rangle$	Cd–H pair	Burchard *et al.* 1997*b*
	$f_1(H)^*$	572(1)	0	$\langle 111 \rangle$	Cd–H pair	Burchard *et al.* 1997*b*

Downloaded from rsta.royalsocietypublishing.org

Downloaded from rsta.royalsocietypublishing.org

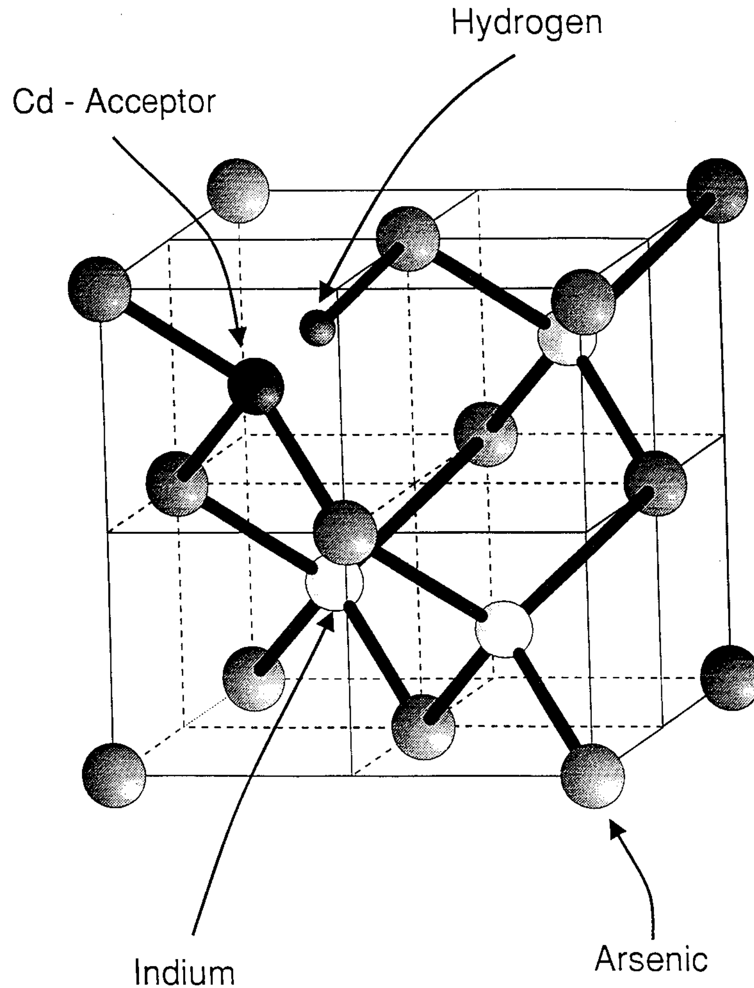

Figure 3. Microscopic configuration of the Cd–H pair in III–V semiconductors following a model proposed by Pajot (1989) for the passivation of Zn acceptors. It is assumed that hydrogen is trapped by the Cd acceptor and occupies a bond-centre-lattice site. The bonding is established between H and the neighbouring group V atom (P,As); the Cd acceptor remains threefold bonded.

tensor corresponds to a $\langle 1\,1\,1 \rangle$ lattice orientation of the Cd–H pairs. In GaAs, InAs, InP and GaP the crystallographic orientation and the stability of the Cd–H pairs support a model proposed by Pajot (1989) that favours H on the bond centre site, forming H–P and H–As bonds instead of an acceptor–hydrogen bond (see figure 3). In GaN complex $f_1(\mathrm{H})$ and $f_1(\mathrm{H})^*$ reflect the wurtzite structure of the material: both are Cd–H pairs, but orientated in different lattice directions (Burchard *et al.* 1997*b*).

PAC experiments not only informs us about the microscopic structure of complexes but also about their stability, which is usually deduced by performing an isochronal furnace annealing programme. Figure 4 shows the temperature dependence of the normalized fraction $f_1(\mathrm{H})$ of Cd–H pairs in GaP. The fraction does

Downloaded from rsta.royalsocietypublishing.org

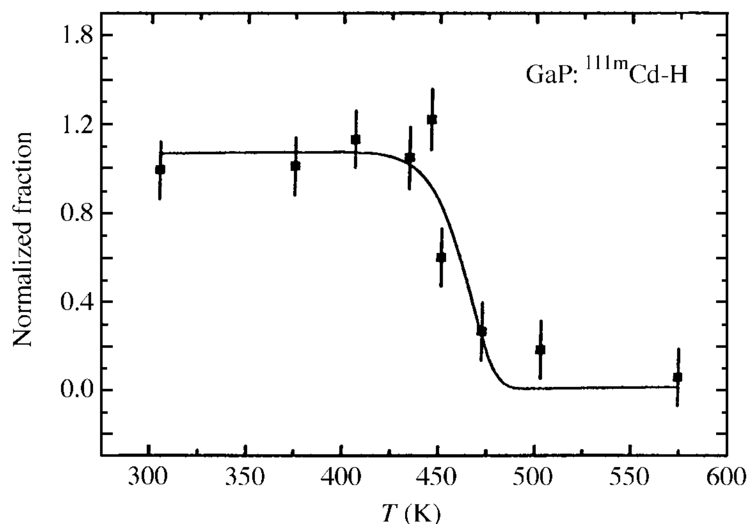

Figure 4. Normalized fraction of Cd–H pairs in GaP. The fit, assuming an attempt frequency of 1×10^{13} s^{-1} and a single-jump mechanism yields a dissociation energy of $E_\mathrm{d} = 1.45(1)$ eV for the Cd–H pairs.

Table 2. *Dissociation energies* E_d *of* Cd–H *pairs* (f_1(H)) *and complexes* (f_2(H)) *formed after plasma charging*

(The results are obtained from least-squares fits to the data, assuming a single-step dissociation process. Parameter ν_0 denotes the attempt frequency. For InP, the stability of the Cd–H pairs seems to depend on the Cd concentration.)

material	complex	E_d (eV)	ν_0 (s^{-1})	remarks
GaAs	$f_1(H)$	1.3(1)	6.6×10^{13}	
GaAs	$f_2(H)$	1.3(1)	6.6×10^{13}	
InAs	$f_1(H)$	1.3(1)	6.6×10^{13}	
InAs	$f_2(H)$	1.0(1)	6.6×10^{13}	
GaP	$f_1(H)$	1.45(1)	1×10^{13}	
InP	$f_1(H)$	1.4(2)	7×10^{13}	Cd-dose: 10^{12} cm^{-2}
InP	$f_1(H)$	2.0(2)	7×10^{13}	Cd-dose: 5–20 $\times 10^{12}$ cm^{-2}

not change at annealing temperatures between 300 and 420 K. Above this temperature range, the dissociation of the pairs is observed (Forkel-Wirth *et al*. 1994). In table 2 the dissociation energy of the Cd–H pairs in plasma-charged materials are given as obtained from least-squares fits to the corresponding data assuming a single-step dissociation. In InP an influence of the Cd background doping concentration on the stability of the Cd–H pairs was found. The data collected up to now indicate a lower effective stability of the Cd–H pairs in InP with lower Cd concentration (1×10^{12} Cd cm^{-2}: $T_\mathrm{d} \approx 420$ K) compared to more heavily doped material (5–20 $\times 10^{12}$ Cd cm^{-2}: $T_\mathrm{d} \approx 600$ K).

The stability of the Cd–H pairs is in agreement with the model of Pajot (1989), which predicts a higher stability for Cd–H pairs in the arsenides than in the phosphides due to the larger binding energy of the As–H bond compared to the P–H

Downloaded from rsta.royalsocietypublishing.org

MATHEMATICAL, PHYSICAL & ENGINEERING SCIENCES
THE ROYAL SOCIETY A
PHILOSOPHICAL TRANSACTIONS OF

bond. However, the fitted results give only an upper limit for the pair dissociation energy, since neither retrapping mechanisms nor the influences of the Fermi level on the stability could be considered. In InP the Cd background concentration clearly influences the stability of the Cd–H pairs: samples implanted with less Cd revealed a dissociation energy for the Cd–H pairs of only 1.4 eV compared to 2.0 eV in more heavily doped crystals. This experimental finding can be explained as a consequence of the Fermi level position. In InP lightly doped with Cd, the complex Cd–H breaks up into Cd^- and H^0, whereas in heavily doped InP it dissociates into Cd^- and H^+, where more energy is required due to the additional Coulomb binding energy. The Cd–H binding energy for lightly Cd-doped InP agrees with that obtained by Pearton *et al*. (1992), who found a dissociation energy of 1.4 eV for Cd–H pairs by CV measurements under reverse bias conditions. Furthermore, the dissociation energy of 1.4 eV of Cd–H in InP fits very well with that obtained for GaP (see table 2). It indicates again that H is trapped at the Cd acceptor, but it establishes a bond to the next-nearest phosphorus atom. Therefore, the binding energy of Cd–H in both InP and GaP is determined by the strength of the H–P bond.

Besides the already identified Cd–H pairs (f_1(H)), two more configurations, f_2(H), $f_2(\mathrm{H})^*$, could be observed under specific experimental conditions in InAs. Detailed experiments in InAs (Forkel-Wirth *et al*. 1994, 1995, 1996; Burchard *et al*. 1997*c*) demonstrate that f_2(H), $f_2(\mathrm{H})^*$ break up at room temperature and the corresponding dissociation energy is $E_\mathrm{d} = 1.0(1)$ eV. When f_2(H) and $f_2(\mathrm{H})^*$ are decreasing, the number of Cd–H pairs (f_1(H)) increases, indicating the transformation of a more complex Cd–H_x or Cd–H-defect configuration into the Cd–H pair.

(*b*) *Hydrogen diffusion in III–V semiconductors*

From the dissociation energy of Cd–H pairs no direct information can be obtained on the free H migration. But in the last few years, the breakthrough in the development of a specific laser ion source (Michin *et al*. 1993) at ISOLDE enables PAC experiments on ^{117}Cd (Burchard *et al*. 1997*e*) which open access to the study of free H migration in III–V semiconductors.

InAs, InP and GaAs have been implanted with 60 keV ^{117}Ag atoms. After the decay of all ^{117}Ag atoms ($T_{1/2} = 73$ s) into ^{117}Cd ($T_{1/2} = 2.4$ h), the radiation damage was removed and ^{117}Cd–H pairs were formed by low-energy H^+ ion implantation. The experimental conditions for annealing and hydrogenation were optimized according to the knowledge obtained by the investigations on ^{111m}Cd. The radioactive acceptor ^{117}Cd decays into ^{117}In, where the PAC measurement takes place. After the chemical transmutation from Cd into In, the PAC probe atom no longer represents an acceptor but either a constituent (InAs,InP) or an isovalent impurity (GaAs). In InAs and InP the H is no longer bound to the PAC probe atom by Coulomb force and diffuses freely. The single diffusion jumps out of the near neighbourhood of ^{117}In can be observed by PAC as a function of temperature.

The first experiments revealed that H is still present in the immediate neighbourhood of the ^{117}In probe atom at 10 and 78 K after the radioactive decay. Fourier transforms of the $R(t)$ spectra clearly reveal two EFGs, and at 10 K the total fraction of probe atoms involved in the hydrogen-correlated complexes is 30% for InP, 60% for GaAs, and 50% for InAs (see figure 5), respectively. The PAC data of the ^{117}In–H configurations are given in table 3. In PAC experiments on ^{111m}Cd, only one

Downloaded from rsta.royalsocietypublishing.org

Table 3. *PAC parameters of* In–H *correlated complexes in III–V semiconductors*
(The PAC measurements were performed by using the PAC probe atom ^{117}Cd → ^{117}In.)

	ν_Q (MHz)	
compound	f_1	f_2
InAs	99(2)	505(2)
GaAs	114(2)	531(2)
InP	97(2)	562(3)

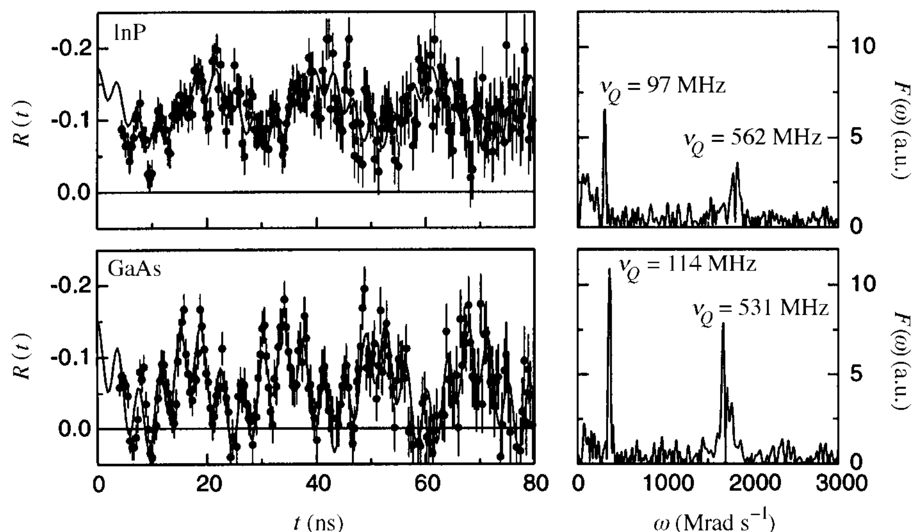

Figure 5. $R(t)$ spectra and the corresponding Fourier transforms of PAC measurements on ^{117}Cd → ^{117}In in low-energy H$^+$-implanted InP and GaAs (Burchard *et al.* 1997*e*). For ^{117}In, each EFG results in only one Fourier peak. The PAC spectra were taken at 10 K.

Cd–H pair was observed under similar conditions. To explain the results on ^{117}In, two different interstitial lattice sites have to be assumed, into which H immediately relaxes after the radioactive decay. At 78 K in GaAs and InAs, the fraction of probe atoms with H in the neighbourhood decreases. This indicates that H already starts diffusing within the short time-window of observation of about 100 ns, which is determined by the lifetime of the isomeric $3/2^+$ state of ^{117}In. The mean time which H needs to perform a first diffusion jump is determined by temperature, and therefore future experiments as a function of measuring temperature will allow determination of the diffusion energy for different hydrogen species.

5. Diffusion of gold in amorphous silicon

In Si, transition-metal impurities like Au or Pt generate electronic states between the valence and conduction bands that lie ‘deep’ in the forbidden gap and present effective recombination centres for free charge carriers. Therefore, dopants like Au

Downloaded from rsta.royalsocietypublishing.org

and Pt are widely used in silicon-device technology to increase transistor switching speed by reducing minority carrier lifetime and diffusion length.

Whereas the diffusion of Au in crystalline Si (c-Si) seems to be already understood (Frank 1991), some open questions still remain in the case of amorphous Si (a-Si). Whereas in c-Si the Au atoms jump from interstitial lattice site to interstitial lattice site, and thus diffuse rapidly, the interstitial diffusion in a-Si is retarded by the presence of intrinsic defects, presumably immobile vacancy-type defects which trap the Au atoms (Frank *et al*. 1996; Horz *et al*. 1996; Frank 1996).

The advantages of using ISOLDE for radiotracer diffusion experiments have been known for a long time (Mehrer 1987). By implanting the radioactive isotopes into the crystal, all problems related to the surface barrier are avoided. Secondly, the Gaussian-shaped concentration profile of the implanted atoms represents a well-defined starting point for the following diffusion measurements. In the case of the experiments on Au diffusion in a-Si (Horz *et al*. 1996; Frank 1996), ISOLDE offers even more advantages: the deposition of a thin transition-metal layer on the amorphous material (which is a common procedure in conventional diffusion experiments) is avoided. This metallic surface layer normally leads to a tremendous decrease in the crystallization temperature (for Au on a-Si from 650 to 160 °C). Furthermore, the Au diffusion can be studied as a function of the Au background concentration over orders of magnitude by introducing the total amount of only 1×10^{11} radioactive ^{195}Au isotopes into samples pre-doped with Au up to 1.7 at.%.

At ISOLDE, ^{195}Hg was implanted into homogeneously Au-doped, relaxed (annealed) and unrelaxed a-Si. After the radioactive decay of ^{195}Hg into ^{195}Au ($T_{1/2}$ = 183 d), the samples were thermally treated and the diffusion profiles were determined by serial Ar^+ beam sectioning and subsequent measurements of the X- and γ-rays emitted by the radiotracers left in the crystals. In figure 6, the ^{195}Au profile after implantation together with two profiles measured after diffusion for a-Si-0.5 at.% Au are shown. From the diffusion-induced changes of the Au profiles, the diffusion coefficient D has been determined. It turned out that, independently of the Au concentration, the ^{195}Au diffusion coefficients obey the Arrhenius laws (see figure 7). For relaxed a-Si, the diffusion enthalpy for Au in a-Si doped with 0–0.1 at.% Au was found to be 2.7 eV, whereas for material doped with 0.2–1.7 at.%, Au 1.9 eV was determined and in unrelaxed material an enthalpy of 1.5 eV was proven.

The experimental results are explained by the authors by a direct diffusion mechanism, where ^{195}Au atoms are temporarily trapped by vacancy-like defects inherent to a-Si (Horz *et al*. 1996; Frank 1996). The diffusion coefficient can be expressed as (Coffa *et al*. 1992)

$$D = D_0^* \exp[-(H^{\mathrm{m}} + H^{\mathrm{b}})/kT],$$

with $D_0^* \propto D_0/C_{\mathrm{t}}$, where D_0 is the pre-exponential factor of the ^{195}Au diffusion in the (hypothetical) trap-free case, H^{m} is the migration enthalpy of Au, C_{t} is the concentration of effective traps, H^{b} is their binding enthalpy, and k is Boltzmann's constant.

In unrelaxed a-Si, mainly shallow traps (H^{b1}) are present, which are tentatively assigned to monovacancies and the corresponding diffusion enthalpy is 1.5 eV. During thermal relaxation the monovacancies become mobile and form di- and tri-vacancies that act as intermediate and deep traps (H^{b2}, H^{b3} with $H^{\mathrm{b1}} < H^{\mathrm{b2}} < H^{\mathrm{b3}}$), respectively. At low Au concentrations the deep traps are not yet saturated, the diffusion

Downloaded from rsta.royalsocietypublishing.org

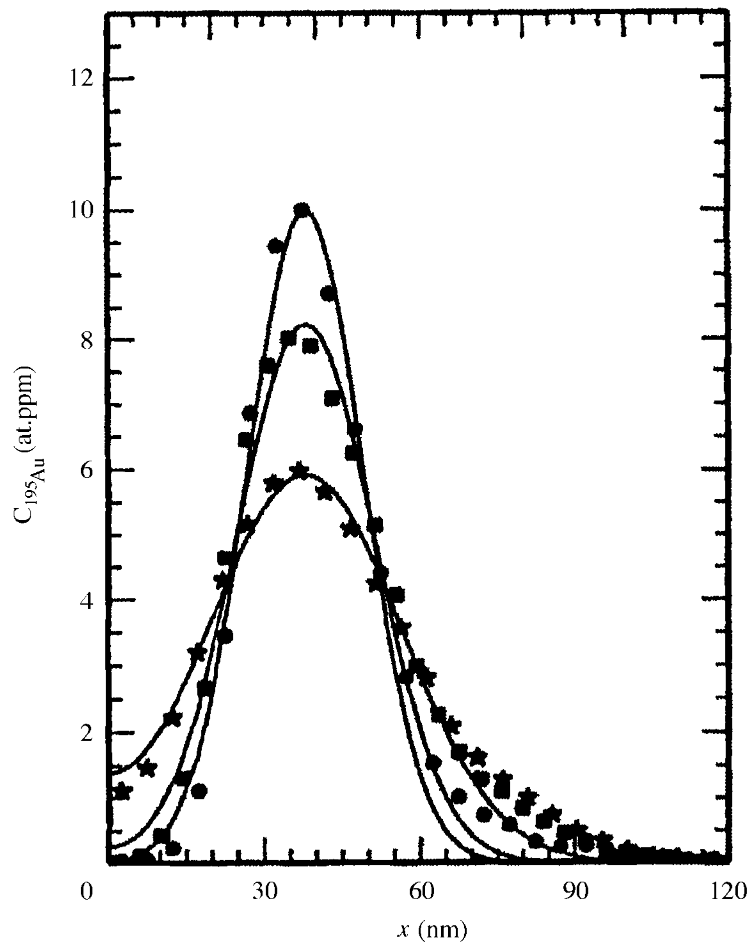

Figure 6. ^{195}Au profiles in unrelaxed a-Si, doped with 0.8 at.% Au, after implantation (•) and after diffusion annealing at 430 °C for 10 s (■) and 23 min (∗), respectively (Horz *et al.* 1996).

is retarded, and the diffusion enthalpy of Au is 2.7 eV. With increasing Au concentration the number of deep traps is reduced by being filled with Au atoms. When all deep traps are saturated, the diffusion is governed by the trapping of Au at intermediate traps (di-vacancy) and the corresponding diffusion enthalpy is smaller (1.9 eV). A complete saturation of the intermediate traps was not reached up to the highest Au concentration (1.7 at.%).

Due to the specific features of ion implantation, it was possible to produce and to investigate Au-doped a-Si samples over a wide range of Au concentrations. Due to the high sensitivity of these experiments, new traps responsible for retarding the Au diffusion have been discovered.

6. Electrical and optical studies of Au and Pt in Si

With the exception of some early experiments (Broser & Franke 1965), the trend to combine radioactive isotopes with the common techniques of semiconductor physics

PHILOSOPHICAL TRANSACTIONS OF THE ROYAL SOCIETY A MATHEMATICAL, PHYSICAL & ENGINEERING SCIENCES

PHILOSOPHICAL TRANSACTIONS OF THE ROYAL SOCIETY A MATHEMATICAL, PHYSICAL & ENGINEERING SCIENCES

Downloaded from rsta.royalsocietypublishing.org

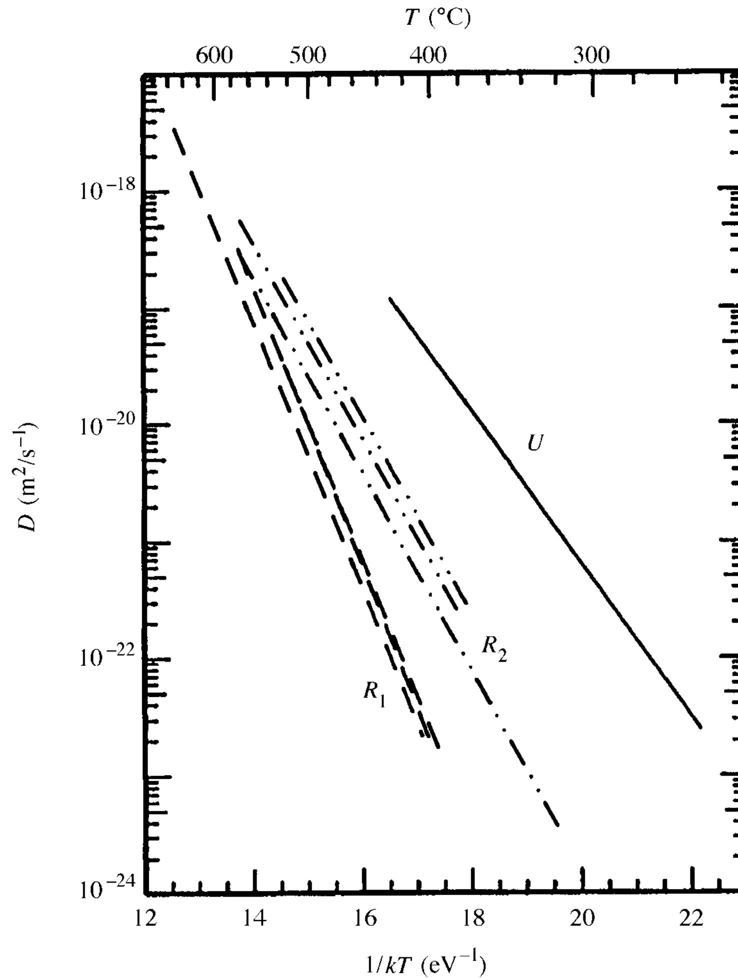

Figure 7. Arrhenius plots of diffusion coefficients of ^{195}Au in a-Si (U: unrelaxed, 0.7 at.% Au, diffusion enthalpy 1.5 eV; R_1: relaxed, 0–0.1 at.% Au, diffusion enthalpy 2.7 eV; R_2: relaxed, 0.2–1.7 at.% Au, diffusion enthalpy 1.9 eV) (Horz *et al*. 1996).

only started at the beginning of the 1990s. The very first experiment combining DLTS and radioactive isotopes was performed by using the system Au and Pt in Si (Petersen & Nielsen 1990, 1992). The aim of this experiment was to shed light on the controversy about Au in Si by comparing it to the already well-understood system of Pt in Si (Ammerlaan & van Oosten 1989, and references therein). For this purpose Si samples were implanted with ^{193}Hg and ^{195}Hg at ISOLDE with 60 keV energy up to a total dose of 10^{12}–10^{13} ions cm^{-2}. The decay schemes of the ground states of the two radioactive isotopes are

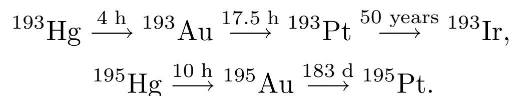

$$^{193}\mathrm{Hg} \xrightarrow{4\ \mathrm{h}} {}^{193}\mathrm{Au} \xrightarrow{17.5\ \mathrm{h}} {}^{193}\mathrm{Pt} \xrightarrow{50\ \mathrm{years}} {}^{193}\mathrm{Ir},$$
$$^{195}\mathrm{Hg} \xrightarrow{10\ \mathrm{h}} {}^{195}\mathrm{Au} \xrightarrow{183\ \mathrm{d}} {}^{195}\mathrm{Pt}.$$

To remove the radiation damage and to diffuse the isotopes deeper into the substrate, the samples were furnace annealed at temperatures between 1070 and 1120 K

Downloaded from rsta.royalsocietypublishing.org

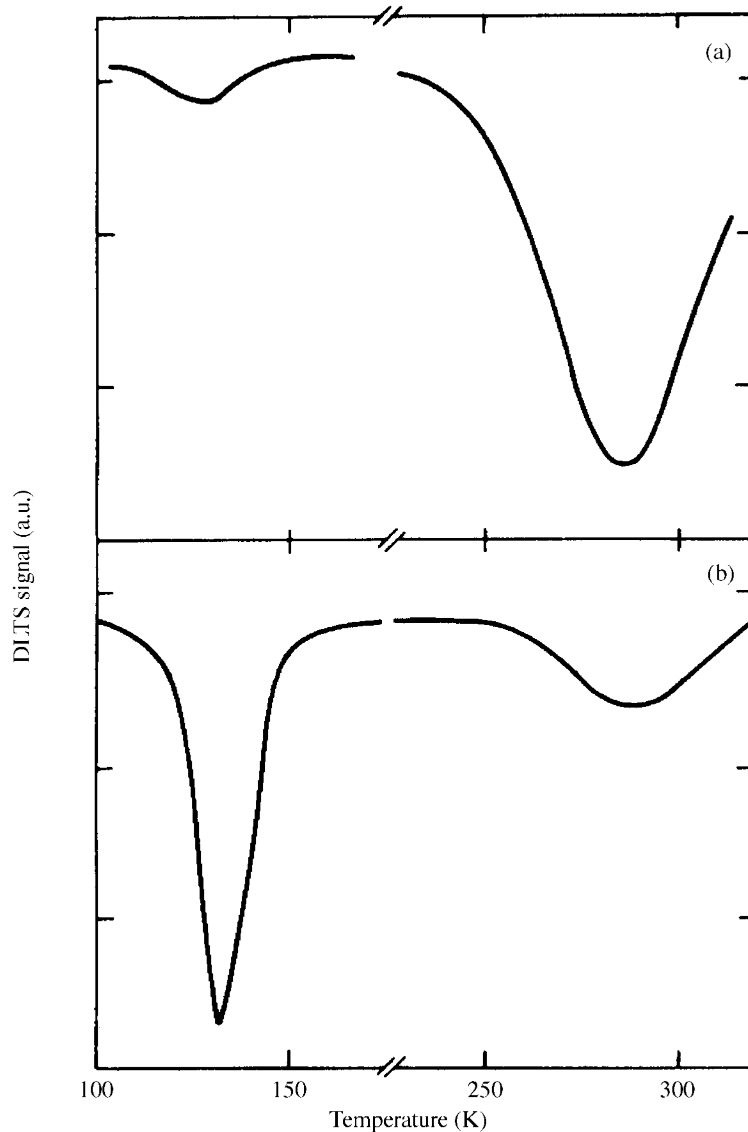

Figure 8. DLTS results for ^{195}Au in p-type Si. The temperature scans were taken shortly after the diffusion (*a*) and two half-lives later (*b*) (Petersen & Nielsen 1990, 1992).

for 0.5–1.5 h. The DLTS measurements were performed within a time-interval of one year, which corresponds to two half-lives of ^{195}Au. The samples doped with ^{193}Pt should remain unchanged. The temperature scans of ^{195}Au-doped n-Si samples shows two electron traps. The relative intensities of the signals change with time, which clearly indicates the transformation of ^{195}Au into ^{195}Pt (see figure 8). The deduced energy levels $E_c - 0.55$ eV and $E_c - 0.22$ eV are in agreement with those reported for Au and Pt acceptors, respectively (Brotherton & Lowther 1980). Since the radioactive decay of ^{195}Au involves only a very low recoil energy (0.3 eV), a site change of the daughter atom can be excluded and ^{195}Pt therefore occupies the same lattice

PHILOSOPHICAL TRANSACTIONS OF THE ROYAL SOCIETY A MATHEMATICAL, PHYSICAL & ENGINEERING SCIENCES

PHILOSOPHICAL TRANSACTIONS OF THE ROYAL SOCIETY A MATHEMATICAL, PHYSICAL & ENGINEERING SCIENCES

Downloaded from rsta.royalsocietypublishing.org

site as the mother isotope ^{195}Au. From EPRS, it is known that Pt is located on substitutional lattice sites (Ammerlaan & van Oosten 1989, and references therein) and the Pt-related energy levels are generated by those substitutional atoms. Therefore, it has to be concluded that the Au acceptor level is caused by substitutional Au impurities. In p-type Si a donor level of $E_v + 0.34$ eV was found for Au which is very close to that of Pt ($E_v + 0.32$ eV), and following the same arguments as in the case of ^{195}Au in n-Si, it has to be assigned to substitutional Au impurities. This first tracer DLTS experiment clearly proved that the Au-levels, which have been known for a long time, are created by substitutional Au impurities. For the first time the radioactive decay was successfully used as a fingerprint for the chemical identification of an impurity, which generates an electrical signal, and nowadays, radiotracer DLTS is widely used (Lang *et al*. 1991, 1992; Achtziger *et al*. 1995; Achtziger & Witthuhn 1995) in semiconductor physics.

Besides electrical radiotracer techniques (DLTS, CV, HE), optical methods like radioactive PLS have been developed during the past few years. Whereas the system Cd in GaAs was studied after off-line implantation of ^{111}In $\rightarrow$ ^{111}Cd in Konstanz (Magerle 1995), the first PLS experiments on Au and Pt in Si were launched at ISOLDE (Henry *et al*. 1996). N-type Si ([P] $= 10^{15}$ cm^{-3}) was implanted with 60 keV ^{191}Hg and ^{195}Hg isotopes. After the decay into ^{191}Pt and ^{195}Au, respectively, the implantation damage was removed by annealing the samples for 5 s at 1173 K. The PLS spectra, however, surprisingly revealed recombination lines which in the literature have been assigned to Ag (for ^{191}Pt) (Nazare *et al*. 1989) and Fe (for ^{195}Au) (DoCarmo *et al*. 1989). But with increasing time, the intensity of the 'Ag'-line decreased with a time constant corresponding to the half-life of ^{191}Pt ($T_{1/2} = 2.9$ d), whereas the same line appears during the radioactive decay of ^{195}Au into Pt (see figure 9). The intensity of the Fe-related lines decreases with the radioactive decay constant of ^{195}Au into ^{195}Pt. Therefore, the PLS line commonly assigned to Fe is most probably caused by Au–Fe complexes, and the former 'Ag' line is found to be Pt related. An unambiguous identification demands more experiments on radioactive Au and Pt in Si. However, already after these few pilot PLS experiments on Au and Pt new results could be obtained on a system which has been studied for nearly 40 years.

7. Site-selective doping of semiconductors

The technical importance of semiconductors is based on their unique feature, that by doping the material with impurity atoms the electrical and optical properties can be tailored over orders of magnitude in a very controlled way. However, in binary (e.g. GaAs) or multi-compound semiconductors (e.g. AlGaAs), it may happen that the dopant impurity occupies lattice sites in more than one sublattice. This amphoteric behaviour of the impurity atoms simultaneously creates acceptors and donors that compensate each other, thus reducing the net charge carrier concentration and leading to an ineffective doping process. But using radioactive atoms, the site selectivity and thus the efficiency of the doping process can be greatly increased. Transmutation doping profits from the change of the chemical nature of the dopant atom caused by the radioactive decay. In the following, two examples of transmutation doping at ISOLDE are given.

Downloaded from rsta.royalsocietypublishing.org

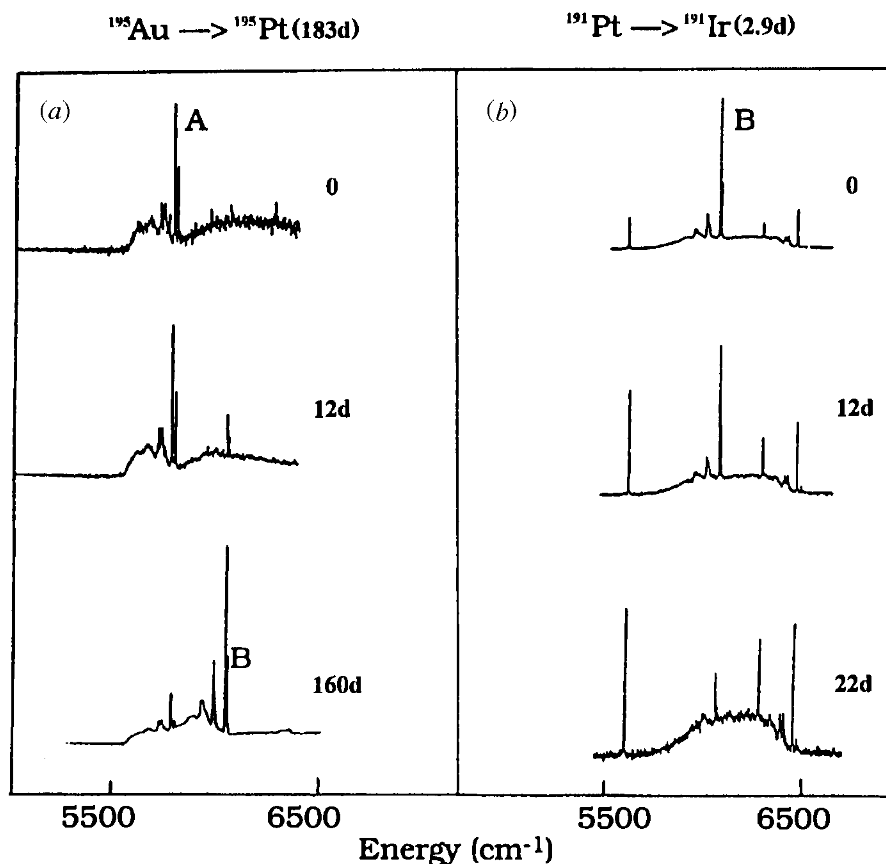

Figure 9. PL spectra of Si doped with ^{191}Pt and ^{195}Au. In both cases a clear time-dependent change of the PL spectra can be observed. The results of the chemical transformation of ^{195}Au into ^{195}Pt are shown in (*a*) and for ^{191}Pt into ^{191}Ir in (*b*) (Henry *et al*. 1996).

Doping a III–V semiconductor with Sn results in the formation of acceptors and donors because the group IV element Sn will occupy lattice sites in the group III sublattice as well as in the group V sublattice. Of course, it is much more effective to force Sn only into one sublattice and one possible technique, transmutation doping, was investigated by MS in 1980 at ISOLDE (Weyer *et al*. 1980). The MS probe atom ^{119}Sn can be produced by the radioactive decay of ^{119}In (group III element) or ^{119}Sb (group V element), and depending on the chemical nature of the mother isotope the daughter Sn should be either mainly located in the In sublattice or in the Sb sublattice. After the implantation of ^{119}In and ^{119}Sb (via ^{119}Xe) into InSb, the isomer shift clearly revealed that ^{119}Sn selectively occupies In lattice sites and Sb lattice sites after ^{119}In and ^{119}Sb implantation, respectively.

In the middle of the 1990s, transmutation doping was once again applied at ISOLDE, this time to increase the doping efficiency of II–VI semiconductors (e.g. ZnSe). This class of semiconductors is characterized by direct band-gaps, covering a broad range of light, from infrared (CdTe) to blue (ZnS). They are used in opto-electronics and ZnSe represents one of the most promising candidates for the blue laser diode. Even the simplest device, a pn-junction, needs a sufficiently high p- and

Downloaded from rsta.royalsocietypublishing.org

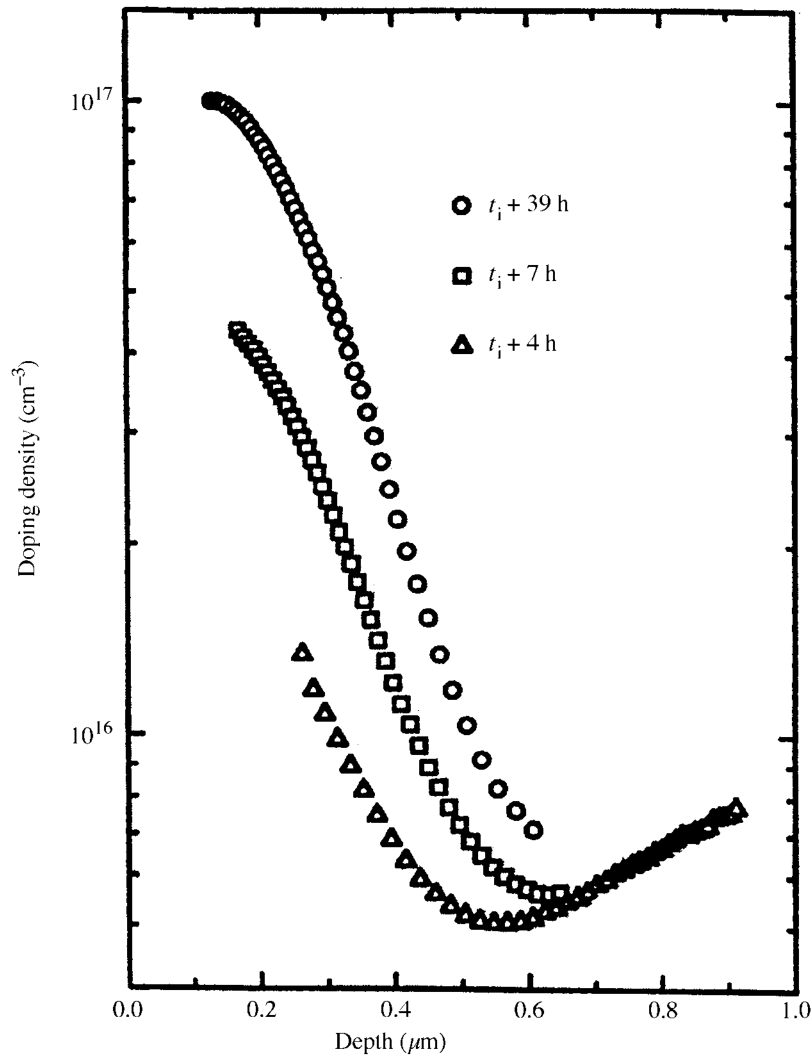

Figure 10. CV measurements of the time-dependent increase of the doping density in p-type CdTe following the transmutation of ^{107}Cd into ^{107}Ag (Bollmann *et al*. 1996*a*, *b*).

n-doped material, but for most of the II–VI semiconductors doping limits exist, which are explained by a compensation mechanism. The impurity Ag is known to act as an acceptor in CdTe when occupying Cd lattice sites. But doping CdTe with Ag by conventional techniques, e.g. by diffusion results in high-resisitivity material: although spark source mass spectroscopy detects between 10^{17} and 10^{19} Ag atoms cm^{-3}, only up to 1% of these Ag atoms act as acceptors (Bollmann *et al*. 1996*a*).

As a result a new approach to doping was tested at ISOLDE: the transmutation

Downloaded from rsta.royalsocietypublishing.org

MATHEMATICAL, PHYSICAL & ENGINEERING SCIENCES
PHILOSOPHICAL TRANSACTIONS OF THE ROYAL SOCIETY A

doping of CdTe by implanting ^{107}Cd, decaying into ^{107}Ag within 6.5 h. The ^{107}Cd ions were implanted at 60 keV up to a dose of 10^{12} cm^{-2} into CdTe. Immediately after the implantation, the radiation damage was removed by annealing the samples at 450 and 600 °C, thus ensuring that ^{107}Cd will be localized in the Cd sublattice after this treatment. Since the recoil energy involved in the β-decay is small, the daughter dopant ^{107}Ag should occupy Cd sublattice sites after the radioactive decay too. Figure 10 shows the results of CV measurements. These are not sensitive to the region close to the surface, and therefore only part of the Gaussian-shaped implantation profile can be observed. The measurements reveal that the implantation profile has broadened due to diffusion and that the number of acceptors is increasing with time, matching the half-life of ^{107}Cd (6.5 h). Finally, nearly all ^{107}Cd atoms have transmuted into ^{107}Ag acceptors, indicating a doping efficiency of nearly 100% (Bollmann *et al*. 1996*a*, *b*).

8. Medium-energy radioactive ion beams in solid state physics

The technical developments at the ISOLDE facility have often contributed to the progress in nuclear solid state physics. The latest example is the development of laser resonance ion sources for Mn and Ag beams (Michin *et al*. 1993; Fedoseyev *et al*. 1997), which offers suitable isotopes for Mössbauer probe atoms (^{57}Mn (Weyer *et al*. 1997)) or for PAC (^{117}Ag $\rightarrow$ ^{117}Cd (Burchard *et al*. 1997*e*)).

The fruitful symbiosis between new technical developments and solid state physics at ISOLDE will continue by using the experimental installation of REX-ISOLDE (Habs *et al*. 1997) to produce medium-energy radioactive beams (E in the range from 300 keV to *ca.* 10 MeV) for solid state physics experiments. These beams will initiate a new generation of 'radioactive' solid state physics experiments at ISOLDE, simply due to the advantage of deeper implantations.

Due to the present ISOLDE implantation energy of only 60 keV, the probe atoms are localized some tens of nanometres below the surface, a fact which might cause some problems. For some combinations of host–lattice and implanted species, the surface acts as a sink for the radioactive atoms, and instead of diffusing into the crystal they preferentially precipitated in the surface region. In semiconductors the implanted probe atoms are localized within the surface space charge region, which hampers experiments within a Schottky diode (Sze 1981). Therefore, experimental techniques such as DLTS or CV are not sensitive to the region close to the surface, and the implanted probe atoms have to be driven deeper into the bulk by diffusion. As a negative consequence, more radioactive ions have to be implanted than are required by the experimental technique itself to compensate for losses during the diffusion step, and in some cases the experiment might even completely fail due to small diffusion coefficients or segregation and precipitation effects. Implantation energies of more than some 100 keV would be necessary to localize the radioactive isotopes deeper in the bulk, outside the surface space charge region.

PAC spectroscopy needs in total only 10^{11}–10^{12} probe atoms to perform an experiment, and, distributed over 1 cm^{-3}, this corresponds to a sensitivity in the range 10^{11}–10^{12} cm^{-3}. However, after a 60 keV implantation the 10^{11}–10^{12} probe atoms are concentrated within an implantation profile of some 10 nm half-width. This corresponds to a local concentration of the probe atoms of the order of 10^{17}–10^{18} cm^{-3} and an involuntary loss of sensitivity of orders of magnitude. By varying the implan-

Downloaded from rsta.royalsocietypublishing.org

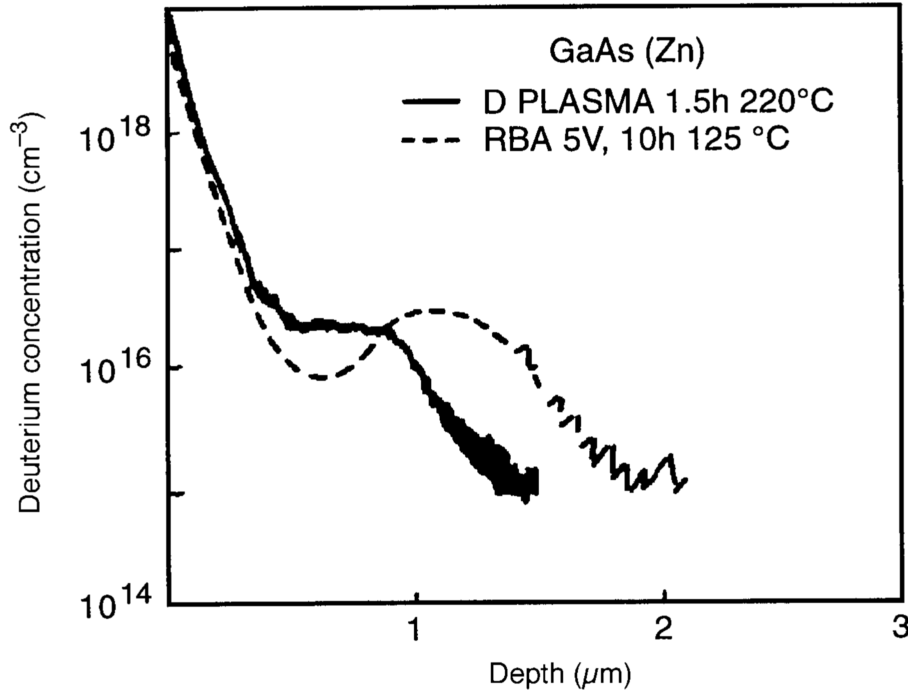

Figure 11. Secondary-ion mass spectroscopy of deuterium in p-type GaAs exposed to a D_2 plasma for 1–5 h at 220 °C and reverse bias annealing ($V_r = 5$ V) for 10 h at 125 °C (Pearton 1994).

tation energy between some hundred kiloelectronvolts and some megaelectronvolts, however, overlapping implantation profiles could be produced, and the resulting local probe atom concentration would be of the order of 10^{15}–10^{16} cm^{-3}. The increase in sensitivity would reveal defect complexes which are not yet PAC-detectable at ISOLDE. Moreover, the possibility of varying the local probe atom concentration between 10^{15} and 10^{19} cm^{-3} would allow the study of the influence of the Fermi level on the formation and stability of defect and impurity complexes.

Many impurities, such as, for example, hydrogen in semiconductors, reveal a non-homogeneous concentration profile (see figure 11). Close to the surface, the H concentration reaches *ca.* 10^{19} cm^{-3}, and with increasing depth the concentration decreases by orders of magnitude. The total depth is typically some micrometres, depending on the background doping. After 60 keV implantation, the PAC probe atoms are localized close to the surface, in the H-rich region. Therefore, all PAC results on H in III–V semiconductors only monitor the first tens of nanometres of the hydrogen profile, whereas implantation energies up to 10 MeV would enable us to investigate the H-passivation mechanism layer by layer and to scan over the whole H profile.

As already mentioned, electrical techniques such as DLTS or CV are only suited for bulk investigations and are not sensitive to the surface region. On the other hand, due to the low ISOLDE implantation energy PAC is only able to monitor the near-surface region. Therefore, a direct comparison between microscopic (PAC) and electrical (DLTS, CV) results is very difficult. The same holds for comparing results of PAC and infrared spectroscopy (IRS). Energies of the order of some megaelectronvolts

PHILOSOPHICAL TRANSACTIONS OF THE ROYAL SOCIETY A MATHEMATICAL, PHYSICAL & ENGINEERING SCIENCES

PHILOSOPHICAL TRANSACTIONS OF THE ROYAL SOCIETY A MATHEMATICAL, PHYSICAL & ENGINEERING SCIENCES

Downloaded from rsta.royalsocietypublishing.org

would solve this problem: the PAC probe atoms could be implanted into the DLTS or CV sensitive region or homogeneously doped samples could be produced which can be investigated by PAC and IRS. Finally, the direct comparison between results of microscopic and macroscopic techniques would become feasible and the conclusions drawn from these different technical approaches would be reinforced.

By passing low-energy beams through stacks of tilted thin foils interspersed with regions of free flight, rather sizeable nuclear polarizations can be obtained. These could then be used for β-NMR, a hyperfine solid state physics technique which depends on the availability of polarized beams of β-emitters. Until now, the technique has been limited to specific probe atoms, which can be either polarized via nuclear reaction (B) or by collinear laser resonance polarization (Li), whereas the tilted foil technique would considerably increase the number of suitable probe atoms.

The study of processes like mechanical wear or chemical erosion by radiotracer techniques are routinely done by direct nuclear reaction activation of the samples. This method cannot be applied to materials such as organics, polymers, or ceramics. A high-energy ^{7}Be beam could extend the application of this valuable technique.

The high-energy beams for solid state physics experiments at ISOLDE will be partly realized by using REX-ISOLDE, a pilot nuclear spectroscopy experiment (Habs *et al*. 1997). High-energy radioactive ion beams are produced by accumulating the 1^{+} ions, delivered by the on-line mass separator ISOLDE within a Penning trap. Afterwards they are converted to highly charged ions in an electron beam ion source (EBIS), and finally accelerated in a linear accelerator up to an energy of 2.2 MeV u^{-1} The ISOLDE solid state physics community will only make use of the highly charged ions, bred by EBIS. After ionization, the beams will be mass-separated and directed back into the already existing ISOLDE beam-line system. From there on, the ions can be sent to several experimental ports, among them an existing high-voltage platform (250–300 kV acceleration voltage) (Lindroos *et al*. 1995), where a moderate post acceleration of some megaelectronvolts in total will be possible.

The installation of REX-ISOLDE is in progress and already in 1998–99 the energetic radioactive beams should be available for the new generation of solid state physics experiments at ISOLDE.

9. Outlook

Solid state physics with radioactive isotopes is a prospering field. Besides the hyperfine techniques and EC, the new radiotracer methods like DLTS, CV, HE or PLS are already appreciated in the semiconductor physics community. To exploit the possibilities of radioactive beams even more efficiently, implantation energies up to some megaelectronvolts would be highly desirable. For some specific experiments such as radioactive EPRs, beam intensities which are a factor 10–100 higher than the present ISOLDE yields would be very helpful.

I would like to cordially thank Manfred Deicher and Angela Burchard from Konstanz University as well as Georg Bollen (ISOLDE/CERN) for scientific discussions and technical support.

References

Achtziger, N. & Witthuhn, W. 1995 *Phys. Rev. Lett.* **75**, 4484.
Achtziger, N., Gottschalck, H., Licht, T., Meier, J., Rueb, M., Reisloehner, U. & Witthuhn, W. 1995 *Appl. Phys. Lett.* **66**, 2370.

Downloaded from rsta.royalsocietypublishing.org

Aeppli, H., Bishop, A. S., Frauenfelder, H., Walter, M. & Zünti, W. 1950 *Phys. Rev.* **82**, 550.
Ammerlaan, C. A. J. & van Oosten, A. B. 1989 *Physica Scr.* T **25**, 342.
Baurichter, A., Deicher, M., Deubler, S., Forkel, D., Plank, H., Wolf, H. & Witthuhn, W. 1989*a* *Appl. Phys. Lett.* **55**, 2301.
Baurichter, A., Deubler, S., Forkel, D., Witthuhn, W. & Wolf, H. 1989*b* *Inst. Phys. Conf. Ser.* **95**, 471.
Baurichter, A., Deicher, M., Deubler, S., Forkel, D., Plank, H., Wolf, H. & Witthuhn, W. 1991 *Appl. Surf. Sci.* **50**, 165.
Baurichter, A., Deicher, M., Deubler, D. , Forkel, D., Meier, J. & Witthuhn, W. 1992 *Mater. Sci. Forum* **83–87**, 593.
Bertschat, H. H., Granzer, H. Haas, H., Kowallik, R. S., Seeger, R. & Zeitz, W.-D. 1997 *Phys. Rev. Lett.* **78**, 342.
Biersack, J. P. & Haggmark, L. G. 1980 *Nucl. Instrum. Meth.* **174**, 257.
Bollmann, J., Wienecke, M., Röhrich, J. & Kerkow, H. 1996*a* *J. Cryst. Growth* **159**, 384.
Bollmann, J., Maass, K., Reinhold, B., Röhrich, J., Wienecke, M. & Forkel-Wirth, D. 1996*b* *J. Cryst. Growth* **161**, 82.
Boyle, A. J. F. & Hall, H. E. 1962 *Rep. Prog. Phys.* **25**, 441.
Broser, I. & Franke, K.-H. 1965 *J. Phys. Chem. Sol.* **26**, 1013.
Brotherton, S. D. & Lowther, J. E. 1980 *Phys. Rev. Lett.* **44**, 606.
Burchard, A., Correia, J., Deicher, M., Fanciulli, M., Forkel-Wirth, D., Henry, M., Magerle, R., Weyer, G. & Ammerlaan, C. 1996 CERN/ISC 96-26, ISC/P81 ADD.1.
Burchard, A., Gelhoff, W., Irmscher, K., Kreissl, J. & Naeser, A. 1997*a* CERN/ISC97-7, ISC/P83 ADD. 1.
Burchard, A., Deicher, M., Forkel-Wirth, D., Haller, E. E., Magerle, R., Prospero, A. & Stötzler, R. 1997*b* In *III–V nitrides* (ed. F. A. Ponce, T. D. Moustakas, I. Akasaki & B. A. Monnemar). Mat. Res. Soc. Symp. Proc., vol. 449, p. 961. Pittsburgh.
Burchard, A., Correia, J. G., Deicher, M., Forkel-Wirth, D., Magerle, R., Prospero, A. & Stötzler, A. 1997*c* *Mat. Sci. For.* **258**–**263**, 945.
Burchard, A., Deicher, M., Forkel-Wirth, D., Haller, E. E., Magerle, R., Prospero, A. & Stötzler, A. 1997*d* *Mat. Sci. For.* **258**–**263**, 1099.
Burchard, A., Deicher, M., Magerle, R., Egenter, A., Spengler, R. & Forkel-Wirth, D. 1997*e* In *7th Int. Conf. Shallow-Level Centers in Semiconducors* (ed. C. A. Ammerlaan & B. Pajot), p. 185. Singapore: World Scientific.
Butz, T. 1993 *Hyp. Int.* **80**, 1079.
Christiansen, J., Heubes, P., Keitel, R., Klinger, W., Löffler, W., Sandner, W. & Witthuhn, W. 1976 *Z. Phys.* B **24**, 177.
Clerjaud, B., Cote, D., Naud, C., Gauneau, M. & Chaplain, R. 1991 *Appl. Phys. Lett.* **59**, 2980.
Coffa, S., Poate, J. M., Jacobson, D. C., Frank, W. & Gustin, W. 1992 *Phys. Rev.* B **45**, 8355.
Conibear, A. B., Leitch, A. W. R. & Ball, C. A. B. 1993 *Phys. Rev.* B **47**, 1846.
Connor, D. 1959 *Phys. Rev. Lett.* **3**, 429.
Correia, G. (and XX others) 1996 CERN/ISC 96-30, ISC/P86.
Daly, S. E., Henry, M. O., Frehill, C. A., Freitag, K., Vianden, R., Rohrlack, G., Forkel, D. 1995 *Mater. Sci. Forum* **196–201**, 1497.
Deicher, M. & Pfeiffer, W. 1994 In *Hydrogen on compound semiconductor, materials science forum* (ed. S. J. Pearton), vols 148–149, p. 481. Aedermannsdorf: Trans Tech Publications.
Deutsch, M. 1951 *Rep. Phys. Soc. Prog. Phys.* **14**, 196.
DoCarmo, M. C., Calao, M. J., Davies, G. & Lightowlers, E. C. 1989 In *Defects in semiconductors* (ed. G. Ferenczo), p. 1497. Aedermannsdorf: Trans Tech Publications.
Fedoseyev, V. N., Batzner, K., Catherall, R., Evensen, A. H. M., Forkel-Wirth, D., Jonsson, O. C., Kugler, E., Lettry, J., Michin, V. I., Ravn, H. L., Weyer, G., and the ISOLDE Collaboration 1997 *Nucl. Instrum. Meth.* B **126**, 88.
Forkel-Wirth, D. (and 12 others) 1994 *Semi-insulating III–V materials* (ed. M. Godlewski), p. 267. Singapore: World Scientific.
Forkel-Wirth, D. (and 13 others) 1995 *Solid State Commun.* **93**, 425.
Forkel-Wirth, D. (and 12 others) 1996 *Mater. Sci. Forum* **196** 201, 987.
Frank, W. 1991 *Def. Diff. Forum* **75**, 121.

PHILOSOPHICAL TRANSACTIONS OF THE ROYAL SOCIETY A MATHEMATICAL, PHYSICAL & ENGINEERING SCIENCES

PHILOSOPHICAL TRANSACTIONS OF THE ROYAL SOCIETY A MATHEMATICAL, PHYSICAL & ENGINEERING SCIENCES

Downloaded from rsta.royalsocietypublishing.org

Frank, W. 1996 DIMAT-96, 5–9 August 1996, Nordkirchen, Germany.
Frank, W., Gustin, W. & Horz, M. 1996 *J. Non-Crystalline Solids* **205**–**207**, 208.
Frauenfelder, H. & Steffen, R. M. 1965. In *Alpha-, beta- and gamma-ray spectroscopy* (ed. K. Siegbahn), p. 997. Amsterdam: North-Holland.
Gebhard, M., Vogt, B. & Witthuhn, W. 1991 *Phys. Rev. Lett.* **67**, 847.
Granzer, H., Bertschat, H. H., Haas, H., Zeitz, W.-D., Lohmüller, J. & Schatz, G. 1996 *Phys. Rev. Lett.* **77**, 4261.
Groh, J. & Hevesey, G. V. 1920 *Ann. Phys.* **65**, 218.
Gwilliam, R., Sealy, B. J. & Vianden, R. 1992 *Nucl. Instrum. Meth.* B **63**, 106.
Haas, A. & Shirley, D. A. 1973 *J. Chem. Phys.* **58**, 3339.
Habs, D. (and 19 others) 1997 *Nucl. Instrum. Meth.* B **126**, 218.
Henry, M. O., Daly, S. E., Frehill, C. A., McGlynn, E., Msdonagh, C., Alves, E., Soares, J. C. & Forkel, D. 1996 In *Proc. of 23rd Int Conf. on Physics of Semiconductors, 4. Berlin, Germany 21–29 July 1996* (eds M. Scheffler & R. Zimmerman).
Hofsäss, H. & Lindner, G. 1991 *Phys. Rep.* **201**, 121.
Hofsäss, H., Winter, S. Jahn, S., Wahl, U. & Recknagel, E. 1992 *Nucl. Instrum. Meth.* B **63**, 83.
Horz, M., Gustin, W., Scharwaechter, P., Frank, W., and the ISOLDE Collaboration 1996 *Int. Conf. on Diffusion in Materials, DIMAT-96, 5–9 August 1996, Nordkirchen, Germany.*
Johnson, N. M., Doland, C., Ponce, F., Walker, J. & Anderson, G. 1991 In *Hydrogen in semiconductors* (ed. M. Stutzmann & J. Chevallier), p. 3. Amsterdam: North-Holland.
Kugler, E. 1993 *Nucl. Instrum. Meth.* B **79**, 322.
Lang, D. V. 1974*a* *J. Appl. Phys.* **45**, 3014.
Lang, D. V. 1974*b* *J. Appl. Phys* **45**, 3023.
Lang, M., Pensl, G., Gebhard, M., Achtziger, N. & Uhrmacher, M. 1991 *Appl. Phys.* A **53**, 95.
Lang, M., Pensl, G., Gebhard, M., Achtziger, N. & Uhrmacher, M. 1992 *Mater. Sci. Forum* **83**–**87**, 1097.
Leitch, A. W. R., Prescha, Th. & Weber, J. 1992 *Phys. Rev.* B **45**,14 400.
Lightowlers, E. C. 1990 In *Growth and characterization of semiconductors* (ed. R. A. Stradling & P. C. Klipstein), p. 135. Bristol: Adam Kilger.
Lindroos, M., Haas, H., de Wachter, J., Pattyn, H. & Langouche, G. 1992 *Nucl. Instrum. Meth.* B **64**, 256.
Lindroos, M., Broude, C., Goldring, G., Haas, H., Hass, M., Richards, P. & Weissmann, L. 1995 *Nucl. Instrum. Meth.* A **361**, 53.
Lohmüller, J., Bertschat, H. H., Granzer, H., Haas, H., Schatz, G. & Zeitz, W. D. 1996 *Hyp. Int.* **97/98**, 203.
Magerle, R. 1995 *Phys. Rev. Lett.* **75**, 1594.
McDonald, R. E. & McNab, T. K. 1976 *Phys. Rev.* B **13**, 39.
Mehrer, H. 1987 *Phys. Status Solidi* A **104**, 247.
Michin, V. I., Fedoseyev, V. N., Kluge, H.-J., Letokhov, V. S., Ravn, H. L., Scheerer, F., Shirakabe, Y., Sundell, S. & Tengblad, O. 1993 *Nucl. Instrum. Meth.* B **73**, 550.
Moriya, N. (and 10 others) 1993 *J. Appl. Phys.* **73**, 4248.
Mössbauer, R. L. 1958*a* *Z. Phys.* **151**, 124.
Mössbauer, R. L. 1958*b* *Naturwissenschaften* **45**, 538.
Nazare, M. H., Carmo, M. C. & Duarte, A. J. 1989 *Mater. Sci. Engng* B **4**, 273.
Pajot, B. 1989 *Inst. Conf. Ser.* **95**, 437.
Pankove, J. I. & Johnson, N. M. (eds) 1991 *Hydrogen in semiconductors, semiconductors and semimetals*, vol. 34. San Diego: Academic Press.
Pavesi, L. & Giannozzi, P. 1992 *Phys. Rev.* B **46**, 4621.
Pearton S. J. (ed.) 1994 Hydrogen in compound semiconductors. *Materials science forum*, vol. 148–149. Aedermannsdorf: Trans Tech Publications.
Pearton, S. J., Hobson, W. S. & Abernathy, C. R. 1992 *Appl. Phys. Lett.* **61**, 1588.
Petersen, J. W. & Nielsen, J. 1990 *Appl. Phys. Lett.* **56**, 1122.
Petersen, J. W. & Nielsen, J. 1992 *Nucl. Instrum. Meth.* B **63**, 186.
Pfeiffer, W., Deicher, M., Keller, R. Magerle, R., Skudlik, H., Wichert, Th., Wolf, H., Forkel, D., Moriya, N. & Kalish, R. 1991*a* *Appl. Surf. Sci.* **50**, 154.
Pfeiffer, W. (and 10 others) 1991*b* *Appl. Phys. Lett.* **58**, 1751.

Downloaded from rsta.royalsocietypublishing.org

Restle, M., Baruth-Ram, K., Quintel, H., Ronning, C., Wahl, U., Jah, S. G. & Hofsäss, H. 1995 *Appl. Phys. Lett.* **66**, 2733.

Schatz, G., Weidinger, A. & Gardener, A. 1996 *Nuclear condensed matter physics: nuclear methods and applications*, 2nd edn. New York: Wiley.

Sze, S. M. 1981 *Physics of semiconductor devices*, 2nd edn. New York: Wiley.

Uggerhoj, E. 1966 *Phys. Lett.* **22**, 382.

van de Walle, C. G. 1991 *Physica* B **170**, 21.

Weyer, G., Degroote, S., Fanciulli, M., Fedoseev, V. N., Langouche, G., Mishin, V. I., Van Bavel, M., Vantomme, A. & the ISOLDE collaboration 1997 *Mat. Sci. For.* **258**–**263**, 437.

Weyer, G., Petersen, J. W., Daamgard, S. & Nielsen, H. L. 1980 *Phys. Rev. Lett.* **44**, 155.

Wichert, Th., Skudlik, H., Deicher, M., Gruebel, G., Keller, R., Recknagel, E. & Song, L. 1987 *Phys. Rev. Lett.* **59**, 2087.

Winter, S. Blässer, S., Hofsäss, H., Jahn, S., Lindner, G., Wahl, U. & Recknagel, E. 1990 *Nucl. Instrum. Meth.* B **48**, 211.